Penerbit Akademia Baru

Journal of Advanced Research in Micro and Nano Engineering

Journal homepage: www.akademiabaru.com/armne.html

ISSN: 2756-8210

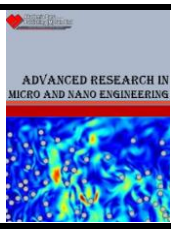

Free Convection Boundary Layer Flow of Jeffrey Nanofluid on a Horizontal Circular Cylinder with Viscous Dissipation Effect

Syazwani Mohd Zokri[1,*], Nur Syamilah Arifin[2], Abdul Rahman Mohd Kasim[3], Mohd Zuki Salleh[3]

[1] Faculty of Computer and Mathematical Sciences, Universiti Teknologi MARA (UiTM) Cawangan Terengganu, Kampus Kuala Terengganu, 21080 Terengganu, Malaysia
[2] Faculty of Computer and Mathematical Sciences, Universiti Teknologi MARA (UiTM) Cawangan Johor, Kampus Pasir Gudang, 81750 Masai, Johor, Malaysia
[3] Centre for Mathematical Sciences, College for Computing and Applied Sciences, Universiti Malaysia Pahang, 26300 Kuantan, Pahang, Malaysia

ABSTRACT

The present study delves into the impact of viscous dissipation and suspended nanoparticles on mixed convection flow of Jeffrey fluid from a horizontal circular cylinder. A concise enlightenment on the separation of boundary layer flow is included and discussed starting from the lower stagnation point flow up to the separation point only. The non-dimensional and non-similarity transformation variables are implemented to transform the dimensional nonlinear partial differential equations (PDEs) into two nonlinear PDEs, and then tackled numerically through the Keller-box method. Representation of tabular and graphical results are executed for velocity and temperature profiles as well as the reduced skin friction coefficient, Nusselt number and Sherwood number to investigate the physical insight of emerging parameters. It was found that the incremented ratio of relaxation to retardation, Deborah number and Eckert number have delayed the boundary layer separation up to $120°$.

Keywords:
Free convection; Jeffrey nanofluid; horizontal circular cylinder; viscous dissipation

Received: 24 Jun. 2020 **Revised: 30 Jul. 2020** **Accepted: 20 Aug. 2020** **Published: 29 Sep. 2020**

1. Introduction

Free convection flow of an incompressible fluid from a horizontal circular cylinder implicates an imperative problem in many industrial applications, for example in handling hot wire and steam pipe. Merkin [1] attempted the initial investigation on free convection boundary layer flow from a horizontal circular cylinder in a viscous fluid. He presented a complete solution of this problem from the lower stagnation point up to the upper stagnation point of circular cylinder using the Blasius and Gortler series expansion methods coupled with an integral method and finite difference scheme. Soon after, he extended the study on a horizontal cylinder of elliptic cross section when the major axis is horizontal and vertical [2]. Both the constant wall temperature and constant heat flux are incorporated. The free convection problem about a heated horizontal cylinder in a porous medium was addressed by Ingham and Pop [3], while Merkin and Pop [4] utilized a similar method as Merkin

* *Corresponding author.*
E-mail address: syazwanizokri@gmail.com

[1] to investigate the constant heat flux condition. Following the works of Merkin [1] and Merkin and Pop [4], the non-Newtonian micropolar fluid was included and thoroughly investigated by Nazar *et al.,* [5] under the constant wall temperature.

Ever since, countless investigations have been conducted from a horizontal circular cylinder in both Newtonian and non-Newtonian fluid. This takes in the published study of Molla *et al.,* [6] who utilized the free convection flow of a viscous fluid past an isothermal horizontal circular cylinder. They supposed that the fluid viscosity is proportional to an inverse linear function of the temperature. They applied the Keller-box method to solve the transformed boundary layer equations starting from the lower stagnation point of the cylinder and then proceeded round the cylinder up to the rear stagnation point. In the subsequent year, Molla *et al.,* [7] continued the investigation by incorporating the internal heat generation effect. The transformed equations were solved numerically using two methods, namely the Keller box method and series solution technique. Again, they observed that the boundary layer proceeds round the cylinder until the upper stagnation point without separating. The surface condition of Newtonian heating was studied by Salleh and Nazar [8] on free convection boundary layer flow in a viscous fluid. Here, the surface heat transfer is assumed to be proportional to the local surface temperature. They concluded that for increasing Prandtl number values, the velocity and temperature profiles were both reduced at the lower stagnation region.

The combined effects of MHD, joule heating and heat generation were then presented by Azim and Chowdhury [9] on free convection flow of a viscous fluid with convective boundary conditions. With the help of Keller-box method, they noted that the skin friction along the surface of the cylinder decreases with increasing magnetic parameter and conjugate conduction parameter. Prasad *et al.,* [10] explored the flow of Jeffrey fluid past a horizontal circular cylinder with suction/injection effect. The numerical computation conducted by the Keller-box method has shown that the Deborah number has a reducing impact on the velocity and Nusselt number, but rising impact on the temperature and skin friction coefficient. Later, Makanda *et al.,* [11] deliberated the radiation effect on MHD free convection flow from a cylinder with partial slip in a non-Darcy porous medium of a Casson fluid. The cylinder surface was heated under constant surface temperature, and the partial slip factor was imposed on the surface for both velocity and temperature. The resulting system of equations were solved using the bivariate quasilinearization method.

Mohamed *et al.,* [12] solved the model of nanofluid due to a horizontal circular cylinder with viscous dissipation effect using the Keller-box method. Authors disclosed that the increase of Brownian motion parameter, thermophoresis parameter, Lewis number and Eckert number has increased the skin friction coefficient and Sherwood number, while the Nusselt number decreases. Rao *et al.,* [13] also applied the Keller-box method to scrutinize the flow of Williamson fluid with Newtonian heating. They reported that the boundary layer separation for skin friction coefficient $(x = 1.5)$ is larger than the Nusselt number $(x = 1.2)$. The convectively heated cylinder in MHD Tangent Hyperbolic Fluid was addressed by Gaffar *et al.,* [14]. It was identified that, for all investigated parameters, the boundary layer flow does not experience singularity.

All the above cited works were restricted to diverse non-Newtonian fluids flow with one of them concentrated on the Jeffrey fluid. However, none of them was identified to deliberate on free convection flow of Jeffrey nanofluid. Motivated by the published works of Mohamed *et al.,* [12] and Dalir [15], the current investigation aims to solve the free convection flow of Jeffrey nanofluid past a horizontal circular cylinder with viscous dissipation effect.

2. Mathematical Formulation

According to Hayat and Ali [16] and Qasim [17], the constitutive equation for the model of Jeffrey fluid is

$$\boldsymbol{\tau} = -p\mathbf{I} + \mathbf{S}, \quad \mathbf{S} = \frac{\mu}{1+\lambda}\left[\mathbf{R}_1 + \lambda_1\left(\frac{\partial \mathbf{R}_1}{\partial t} + \mathbf{V}.\nabla\right)\mathbf{R}_1\right]$$

where $\boldsymbol{\tau}$, $\mathbf{I}$, $\mathbf{S}$, p and μ are the Cauchy stress tensor, identity tensor, extra stress tensor, pressure and dynamic viscosity. Furthermore, the material parameters of the Jeffrey fluid are symbolized as λ and λ_1 while $\mathbf{R}_1 = (\nabla \mathbf{V}) + (\nabla \mathbf{V})'$ is the Rivlin-Ericksen tensor. This model is developed with the purpose of extending the Maxwell model. The retardation time parameter which appears in Maxwell model is specifically corrected with the time derivative of the strain rate, for which it can measure the required time for the material to react to the deformation.

A steady, two-dimensional and laminar flow of the Jeffrey nanofluid model with uniform ambient temperature T_∞ and concentration C_∞ is investigated due to a horizontal circular cylinder. The cylinder is heated at the same constant temperature T_w and concentration C_w, as exhibited in the flow diagram of Figure 1.

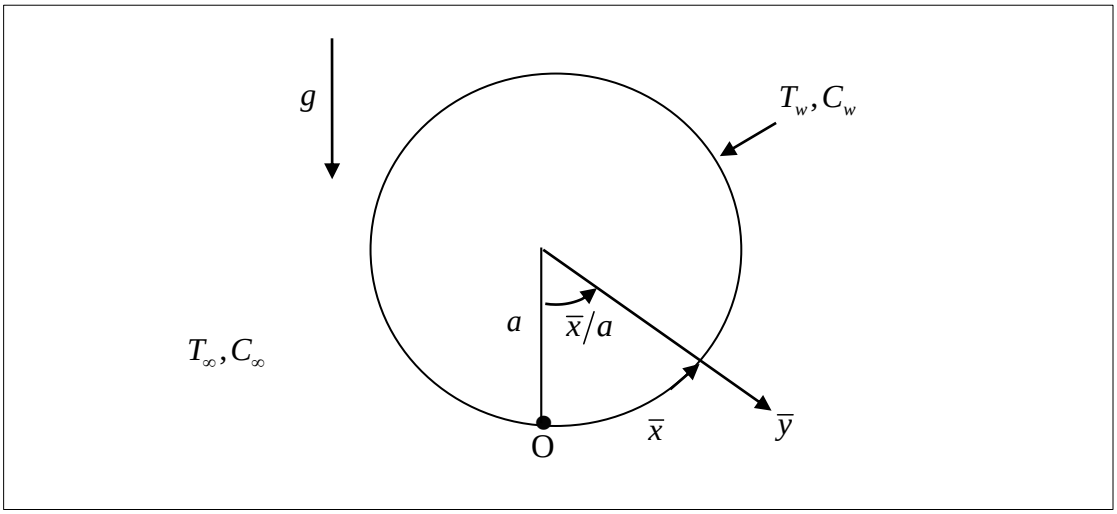

Fig. 1. Schematic diagram of free convection flow in Jeffrey fluid passing over a horizontal circular cylinder

The respective $\bar{x}-$ and $\bar{y}-$ coordinates are implicated throughout the surface of the cylinder from the lowest point, $\bar{x} = 0$ and vertical to it, with a and g being the radius of the circular cylinder and gravitational acceleration, respectively. The amalgamation influences of the viscous dissipation and mixed convection are also scrutinized. The law of conservation (after applying the boundary layer approximations) are proposed as the following:

$$\frac{\partial \bar{u}}{\partial \bar{x}} + \frac{\partial \bar{v}}{\partial \bar{y}} = 0, \tag{1}$$

$$\bar{u}\frac{\partial \bar{u}}{\partial \bar{x}}+\bar{v}\frac{\partial \bar{u}}{\partial \bar{y}}=\frac{\nu}{1+\lambda}\left[\frac{\partial^2 \bar{u}}{\partial \bar{y}^2}+\lambda_1\left(\bar{u}\frac{\partial^3 \bar{u}}{\partial \bar{x}\partial \bar{y}^2}+\bar{v}\frac{\partial^3 \bar{u}}{\partial \bar{y}^3}-\frac{\partial \bar{u}}{\partial \bar{x}}\frac{\partial^2 \bar{u}}{\partial \bar{y}^2}+\frac{\partial \bar{u}}{\partial \bar{y}}\frac{\partial^2 \bar{u}}{\partial \bar{x}\partial \bar{y}}\right)\right]+ g\beta_T(T-T_\infty)\sin\frac{\bar{x}}{a}+g\beta_C(C-C_\infty)\sin\frac{\bar{x}}{a}, \tag{2}$$

$$\bar{u}\frac{\partial T}{\partial \bar{x}}+\bar{v}\frac{\partial T}{\partial \bar{y}}=\alpha\frac{\partial^2 T}{\partial \bar{y}^2}+\frac{\nu}{C_p(1+\lambda)}\left[\left(\frac{\partial \bar{u}}{\partial \bar{y}}\right)^2+\lambda_1\left(\bar{u}\frac{\partial \bar{u}}{\partial \bar{y}}\frac{\partial^2 \bar{u}}{\partial \bar{x}\partial \bar{y}}+\bar{v}\frac{\partial \bar{u}}{\partial \bar{y}}\frac{\partial^2 \bar{u}}{\partial \bar{y}^2}\right)\right]+ \tau\left[D_B\frac{\partial C}{\partial \bar{y}}\frac{\partial T}{\partial \bar{y}}+\frac{D_T}{T_\infty}\left(\frac{\partial T}{\partial \bar{y}}\right)^2\right], \tag{3}$$

$$\bar{u}\frac{\partial C}{\partial \bar{x}}+\bar{v}\frac{\partial C}{\partial \bar{y}}=D_B\frac{\partial^2 C}{\partial \bar{y}^2}+\frac{D_T}{T_\infty}\frac{\partial^2 T}{\partial \bar{y}^2} \tag{4}$$

In the above equations, the ratio of heat capacity of the nanoparticle to the fluid and the velocity outside the boundary layer are denoted as $\tau=(\rho c)_p/(\rho c)_f$ and $\bar{u}_e(x)=U_\infty\sin(\bar{x}/a)$, respectively, whereas the velocity components along the $\bar{x}-$ and $\bar{y}-$ coordinates are symbolized as $\bar{u}$ and $\bar{v}$, respectively. Besides, the respective ratio of relaxation to retardation times, relaxation time, thermal expansion, concentration expansion, thermal diffusivity, kinematic viscosity, fluid density, local concentration, specific heat capacity at a constant pressure, local temperature, Brownian diffusion coefficient and thermophoretic diffusion coefficient are indicated as λ, λ_1, β_T, β_C, α, ν, ρ, C, C_p, T, D_B and D_T. Eq. (1) to (4) are subjected to the following boundary conditions

$$\begin{aligned}&\bar{u}(\bar{x},0)=0,\ \bar{v}(\bar{x},0)=0,\ T(\bar{x},0)=T_w,\ C(\bar{x},0)=C_w \text{ at } \bar{y}=0\\ &\bar{u}(\bar{x},\infty)\to 0,\ \bar{v}(\bar{x},\infty)\to 0,\ T(\bar{x},\infty)\to T_\infty,\ C(\bar{x},\infty)\to C_\infty \text{ as } \bar{y}\to\infty\end{aligned} \tag{5}$$

The above mathematical model can be further non-dimensionlized using the subsequent variables

$$x=\frac{\bar{x}}{a},\ y=Gr_x^{1/4}\frac{\bar{y}}{a},\ u=\frac{a}{\nu}Gr_x^{-1/2}\bar{u},\ v=\frac{a}{\nu}Gr_x^{-1/4}\bar{v},\ \theta(\eta)=\frac{T-T_\infty}{T_w-T_\infty},\ \phi(\eta)=\frac{C-C_\infty}{C_w-C_\infty} \tag{6}$$

Using Eq. (6), Eq. (1) to (5) yield

$$\frac{\partial u}{\partial x}+\frac{\partial v}{\partial y}=0 \tag{7}$$

$$u\frac{\partial u}{\partial x}+v\frac{\partial u}{\partial y}=\frac{1}{1+\lambda}\left[\frac{\partial^2 u}{\partial y^2}+\lambda_2\left(u\frac{\partial^3 u}{\partial x\partial y^2}-\frac{\partial u}{\partial x}\frac{\partial^2 u}{\partial y^2}+v\frac{\partial^3 u}{\partial y^3}+\frac{\partial u}{\partial y}\frac{\partial^2 u}{\partial x\partial y}\right)\right]+(\theta+N\phi)\sin x \tag{8}$$

$$u\frac{\partial\theta}{\partial x}+v\frac{\partial\theta}{\partial y}=\frac{1}{\Pr}\frac{\partial^2\theta}{\partial y^2}+Nb\frac{\partial\phi}{\partial y}\frac{\partial\theta}{\partial y}+Nt\left(\frac{\partial\theta}{\partial y}\right)^2+\frac{Ec}{(1+\lambda)}\left[\left(\frac{\partial u}{\partial y}\right)^2+\lambda_2\left(u\frac{\partial u}{\partial y}\frac{\partial^2 u}{\partial x\partial y}+v\frac{\partial u}{\partial y}\frac{\partial^2 u}{\partial y^2}\right)\right] \tag{9}$$

$$u\frac{\partial\phi}{\partial x}+v\frac{\partial\phi}{\partial y}=\frac{1}{Le\,\Pr}\left(\frac{\partial^2\phi}{\partial y^2}+\frac{Nt}{Nb}\frac{\partial^2\theta}{\partial y^2}\right) \tag{10}$$

$$\begin{aligned}&u(x,0)=0,\quad v(x,0)=0,\quad \theta(x,0)=1,\quad \phi(x,0)=1\quad \text{at}\quad y=0\\&u(x,\infty)\to 0,\quad v(x,\infty)\to 0,\quad \theta(x,\infty)\to 0,\quad \phi(x,\infty)\to 0\quad \text{as}\quad y\to\infty\end{aligned} \tag{11}$$

In consequence of the above equations, we let $\Pr$, λ_2, Ec, γ, Gr_x, Re, N, Nb, Le and Nt be the Prandtl number, Deborah number, Eckert number, mixed convection parameter, Grashof number, Reynolds number, concentration buoyancy parameter, Brownian motion parameter, Lewis number and thermophoresis diffusion parameter, which can be expressed as below

$$\Pr=\frac{\nu}{\alpha},\ \lambda_2=\frac{\lambda_1 Gr_x^{1/2}\nu}{a^2},\ Ec=\frac{\nu^2 Gr_x}{a^2 C_p\left(T_w-T_\infty\right)},\ Gr_x=\frac{g\beta_T(T_w-T_\infty)a^3}{\nu^2},\ \mathrm{Re}=\frac{U_\infty a}{\nu},$$
$$N=\frac{\beta_C\left(C_w-C_\infty\right)}{\beta_T\left(T_w-T_\infty\right)},\ Nb=\frac{\tau D_B(C_w-C_\infty)}{\nu},\ Le=\frac{\alpha}{D_B},\ Nt=\frac{\tau D_T(T_w-T_\infty)}{\nu T_\infty}$$

Next, we look for these variables to solve Eq. (7) to (11): $\psi=xf(x,y)$, $\theta=\theta(x,y)$ and $\phi=\phi(x,y)$, in which the stream function, ψ is represented by $u=\partial\psi/\partial y$ and $v=-\partial\psi/\partial x$. Now, the satisfaction of Eq. (7) is automatically achieved and the resulting PDEs together with the related boundary conditions are

$$\begin{aligned}&\frac{1}{1+\lambda}f'''-\left(f'\right)^2+ff''+\frac{\sin x}{x}\left[\gamma\left(\theta+N\phi\right)+\cos x\right]+\frac{\lambda_2}{1+\lambda}\left[\left(f''\right)^2-ff^{(iv)}\right]=\\&x\left[f'\frac{\partial f'}{\partial x}-f''\frac{\partial f}{\partial x}+\frac{\lambda_2}{1+\lambda}\left(f'''\frac{\partial f'}{\partial x}+f^{(iv)}\frac{\partial f}{\partial x}-f''\frac{\partial f''}{\partial x}-f'\frac{\partial f'''}{\partial x}\right)\right]\end{aligned} \tag{12}$$

$$\begin{aligned}&\frac{1}{\Pr}\theta''+f\theta'+Nb\theta'\phi'+Nt\left(\theta'\right)^2=\\&x\left[f'\frac{\partial\theta}{\partial x}-\theta'\frac{\partial f}{\partial x}-x\frac{Ec}{(1+\lambda)}\left(\left(f''\right)^2+\lambda_2\left(xff''\frac{\partial f''}{\partial x}+f'\left(f''\right)^2-xff''f'''\frac{\partial f}{\partial x}-ff''f'''\right)\right)\right]\end{aligned} \tag{13}$$

$$\phi''+Le\,\Pr\,f\phi'+\frac{Nt}{Nb}\theta''=xLe\,\Pr\left[f'\frac{\partial\phi}{\partial x}-\phi'\frac{\partial f}{\partial x}\right] \tag{14}$$

$$\begin{aligned}&f(x,0)=0,\quad f'(x,0)=0,\quad \theta(x,0)=1,\quad \phi(x,0)=1\ \text{ at }\ y=0\\&f'(x,\infty)\to\frac{\sin x}{x},\quad f''(x,\infty)\to 0,\quad \theta(x,\infty)\to 0,\quad \phi(x,\infty)\to 0\ \text{ as }\ y\to\infty\end{aligned} \tag{15}$$

Note that primes infer the differentiation with respect to the variable y. Also, we found that Eq. (12) to (15) can be reduced to the mixed convection Newtonian fluid as reported by Mohamed *et al.,* [18], provided the absence of the Jeffrey fluid $(\lambda = \lambda_2 = 0)$ and nanofluid $(Nt = Nb = Le = N = 0)$ parameters. At the vicinity of the lower stagnation point $(x \approx 0)$, the preceding equations (Eq. (12) to (15)) give rise to the succeeding ordinary differential equations:

$$\frac{1}{1+\lambda} f''' + ff'' - (f')^2 + 1 + \gamma(\theta + N\phi) + \frac{\lambda_2}{1+\lambda}\left[(f'')^2 - ff^{(iv)}\right] = 0, \tag{16}$$

$$\frac{1}{\Pr}\theta'' + f\theta' + Nb\theta'\phi' + Nt(\theta')^2 = 0 \tag{17}$$

$$\phi'' + Le\,\Pr\, f\phi' + \frac{Nt}{Nb}\theta'' = 0 \tag{18}$$

$$\begin{aligned} &f(0) = 0,\ \ f'(0) = 0,\ \ \theta(0) = 1,\ \ \phi(0) = 1 \\ &f'(\infty) \to 1,\ \ f''(\infty) \to 0,\ \ \theta(\infty) \to 0,\ \ \phi(\infty) \to 0 \end{aligned} \tag{19}$$

The non-appearance of parameter Ec in Eq. (17) clearly signifies that the profiles of velocity, temperature and concentration are no longer being influenced by Ec at the stagnation point of the cylinder. Further, the local Nusselt and Sherwood numbers are exemplified as follows

$$C_{fr} = \frac{S_w}{\rho_f U_\infty^2},\ S_w = \frac{\mu}{1+\lambda}\left[\frac{\partial \bar{u}}{\partial \bar{y}} + \lambda_1\left(\bar{u}\frac{\partial^2 \bar{u}}{\partial \bar{x}\partial \bar{y}} + \bar{v}\frac{\partial^2 \bar{u}}{\partial \bar{y}^2}\right)\right]_{\bar{y}=0},\ Nu_x = \frac{aq_w}{k(T_w - T_\infty)},\ q_w = -k\left(\frac{\partial T}{\partial \bar{y}}\right)_{\bar{y}=0} \text{ and}$$

$$Sh_x = \frac{aj_w}{D_B(C_w - C_\infty)},\ j_w = -D_B\left(\frac{\partial C}{\partial \bar{y}}\right)_{\bar{y}=0} \tag{20}$$

The reduced Nusselt and Sherwood numbers are now given by

$$C_{fr}Gr_x^{1/4} = \frac{x}{1+\lambda} f''(x,0),\ Nu_x Gr_x^{-1/4} = -\theta'(x,0) \text{ and } Sh_x Gr_x^{-1/4} = -\phi'(x,0) \tag{21}$$

3. Results and Discussion

The non-linear PDEs in Eq. (12) to (14) with the respective boundary conditions in Eq. (15) are treated through the Keller-box method. The numerical solutions start at the lower stagnation point, $x = 0°$ with initial profiles being given by Eq. (16) to Eq. (18) accompanied by boundary conditions (19) and then proceed round the circular cylinder up to the separation point $x = 120°$. The step size of $\Delta x = \Delta y = 0.01$ and the boundary layer thickness, $y_\infty = 4$ to 6 are implemented to obtain the numerical results. The results of this study are comprehensively explored and discussed for diverse values of dimensionless governing equations λ, λ_2 and Ec, as illustrated in Figures 1 to 9.

In order to authenticate the engaged numerical method, the comparative benchmark of the $C_{fr}Gr_x^{1/4}$ and $Nu_xGr_x^{-1/4}$ values against position of x are presented through Tables 1 and 2. The limiting results of the current study are matched with the tabulated values of Merkin [1], Nazar *et al.,* [5], Molla *et al.,* [7], Azim and Chowdhury [19] and Mohamed *et al.,* [12], who applied the Keller-box method in solving the free convection flow of viscous, micropolar and nanofluid. A proper match among the comparative values of both tables has manifestly validated the present results. Furthermore, it can be concluded from the comparative values that the $C_{fr}Gr_x^{1/4}$ rises to a maximum value before declining to a finite value, while the $Nu_xGr_x^{-1/4}$ decelerates with increasing position of x.

The graph for velocity $f'(y)$, temperature $\theta(y)$ and concentration $\phi(y)$ profiles are portrayed in Figures 2 to 4 for different values of λ and λ_2. Initially, a rise in λ is noticed to boost the velocity profile; however, the velocity profile starts to deteriorate as the momentum boundary layer thickness increases. Instead, a reversal graph trend is observed for increasing λ_2 values. It is perceived that λ_2 displays a trivial effect at the cylinder surface, but the effect comes to be highly substantial as the thickness of boundary layer increases up to the freestream. Moreover, with increasing value of λ, the decrease in temperature profile is found to be slightly significant than the decrease in concentration profile. This outcome goes in the same way as for rising λ_2 values, where a slight significant increase in temperature rather than the concentration profile is spotted. These profiles also decline continuously towards the freestream following the escalation of the boundary layer thickness.

Salient features of skin friction coefficient $C_{fr}Gr_x^{1/4}$, Nusselt number $Nu_xGr_x^{-1/4}$ and Sherwood number $Sh_xGr_x^{-1/4}$ are portrayed in Figures 5 to 10 for various values of λ, λ_2 and Ec. These figures have demonstrated that the boundary layer separation had occurred at $x=120°$, regardless of the varied parameter values. Figures 5 to 7 demonstrate that the $C_{fr}Gr_x^{1/4}$ is a lessening function of λ and a rising function of λ_2, while both the $Nu_xGr_x^{-1/4}$ and $Sh_xGr_x^{-1/4}$ perform reversely. It is observed that the heat and nanoparticle concentration transfer rates reduce sequentially as the tangential coordinate value, x increases. Figures 8 to 10 exhibit that, Ec enunciates a rising impact over the $C_{fr}Gr_x^{1/4}$ and the $Sh_xGr_x^{-1/4}$, but a lessening impact over the $Nu_xGr_x^{-1/4}$. Here, the reversal behaviour of heat transfer transpires as the $Nu_xGr_x^{-1/4}$ values become negative by virtue of escalating Ec from 0 to 2. Besides, the impact of Ec for each profile is not plotted here because the graph generates a unique solution. Mathematically, this can also be connected with discontinuation of Ec in the energy equation in Eq. (17), which subsequently leads to a unique solution of $C_{fr}Gr_x^{1/4}$, $Nu_xGr_x^{-1/4}$ and $Sh_xGr_x^{-1/4}$ at $x=0°$.

Table 1
Comparative values of $C_{fr}Gr_x^{1/4}$ for different values of x when $\lambda = 0,\ \lambda_2 \to 0$ (very small), $N = Ec = Nb = Nt = Le = 0$ and $\Pr = 1$

$C_{fr}Gr_x^{1/4}$						
x	Merkin [1]	Nazar *et al.,* [5]	Molla *et al.,* [7]	Azim and Chowdhury [19]	Mohamed *et al.,* [12]	Present
0	0.0000	0.0000	0.0000	0.0000	0.0000	0.0000
$\pi/6$	0.4151	0.4148	0.4145	0.4139	0.4121	0.4120
$\pi/3$	0.7558	0.7542	0.7539	0.7528	0.7538	0.7507
$\pi/2$	0.9579	0.9545	0.9541	0.9526	0.9563	0.9554
$2\pi/3$	0.9756	0.9698	0.9696	0.9678	0.9743	0.9728
$5\pi/6$	0.7822	0.7740	0.7739	0.7718	0.7813	0.7761
π	0.3391	0.3265	0.3264	0.3239	0.3371	0.3302

Table 2
Comparative values of $Nu_xGr_x^{-1/4}$ for different values of x when $\lambda = 0,\ \lambda_2 \to 0$ (very small), $N = Ec = Nb = Nt = Le = 0$ and $\Pr = 1$

$Nu_xGr_x^{-1/4}$						
x	Merkin [1]	Nazar *et al.,* [5]	Molla *et al.,* [7]	Azim and Chowdhury [19]	Mohamed *et al.,* [12]	Present
0	0.4214	0.4214	0.4214	0.4216	0.4214	0.4214
$\pi/6$	0.4161	0.4161	0.4161	0.4163	0.4163	0.4162
$\pi/3$	0.4007	0.4005	0.4005	0.4006	0.4008	0.4009
$\pi/2$	0.3745	0.3741	0.3740	0.3742	0.3744	0.3743
$2\pi/3$	0.3364	0.3355	0.3355	0.3356	0.3364	0.3363
$5\pi/6$	0.2825	0.2811	0.2812	0.2811	0.2824	0.2814
π	0.1945	0.1916	0.1917	0.1912	0.1939	0.1932

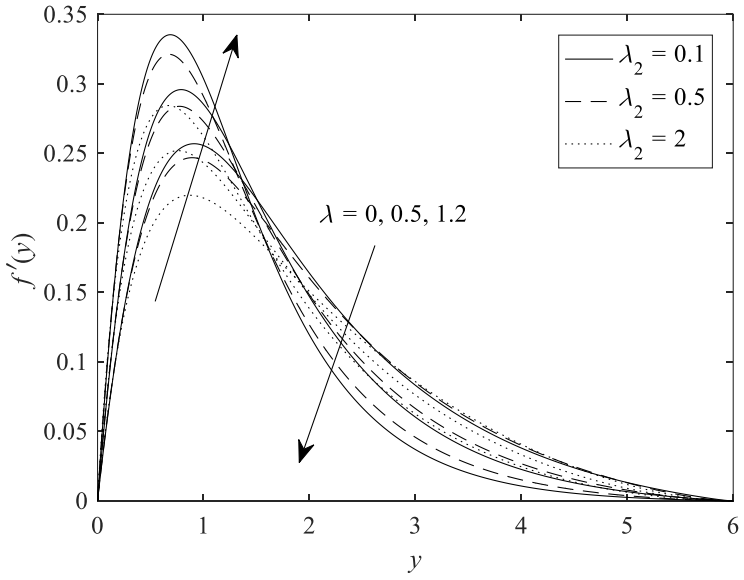

Fig. 2. Variation of $f'(y)$ for several values of λ and λ_2 when $N = Nb = Nt = Ec = 0.1,\ Le = 10$ and $\Pr = 7$

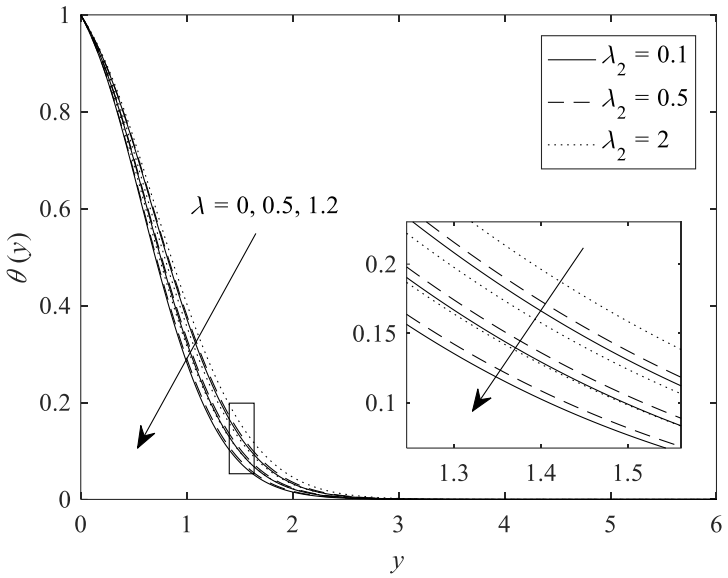

Fig. 3. Variation of $\theta(y)$ for several values of λ and λ_2 when $N = Nb = Nt = Ec = 0.1$, $Le = 10$ and $\Pr = 7$

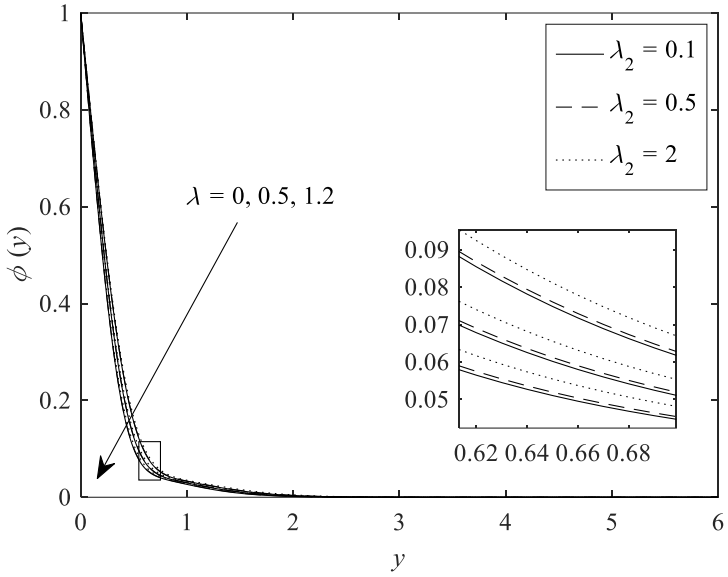

Fig. 4. Variation of $\phi(y)$ for several values of λ and λ_2 when $N = Nb = Nt = Ec = 0.1$, $Le = 10$ and $\Pr = 7$

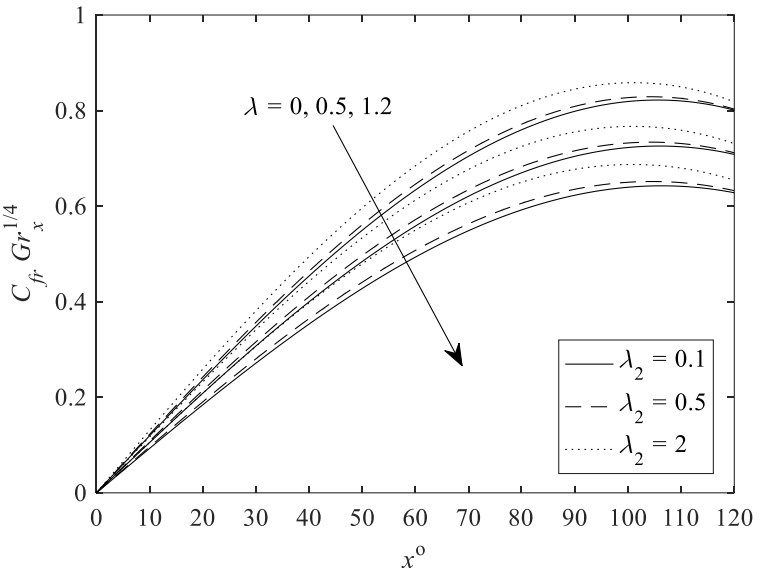

Fig. 5. Variation of $C_{fr}Gr_x^{1/4}$ for several values of λ and λ_2 when $N = Nb = Nt = Ec = 0.1,\ Le = 10$ and $\Pr = 7$

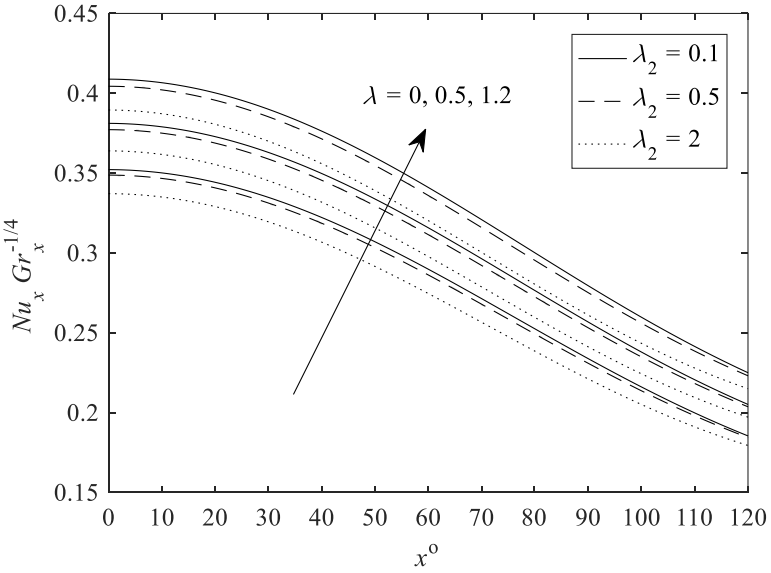

Fig. 6. Variation of $Nu_x Gr_x^{-1/4}$ for several values of λ and λ_2 when $N = Nb = Nt = Ec = 0.1,\ Le = 10$ and $\Pr = 7$

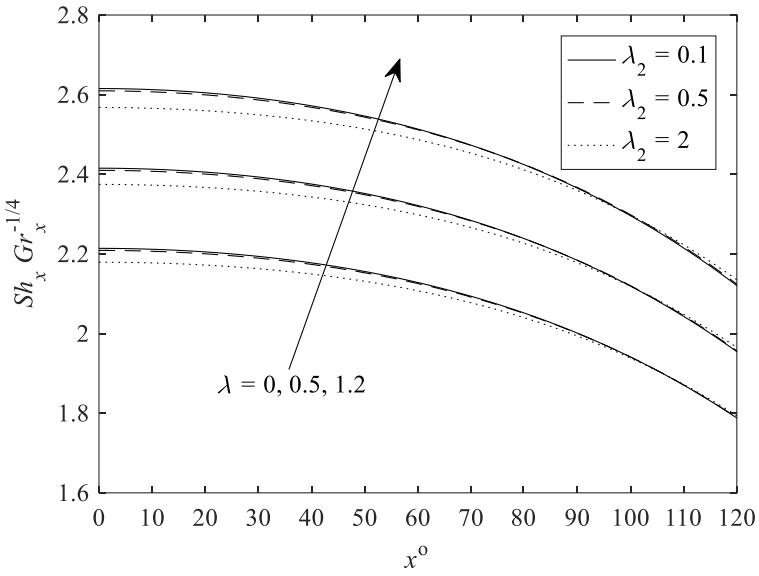

Fig. 7. Variation of $Sh_x Gr_x^{-1/4}$ for several values of λ and λ_2 when $N = Nb = Nt = Ec = 0.1,\ Le = 10$ and $\Pr = 7$

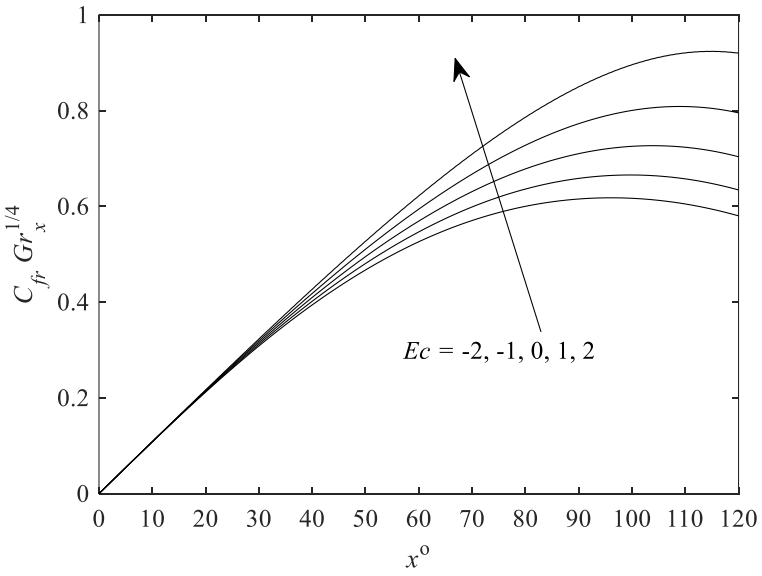

Fig. 8. Variation of $C_{fr} Gr_x^{1/4}$ for several values of Ec when $\lambda = \lambda_2 = 0.5,\ N = Nb = Nt = 0.1,\ Le = 10$ and $\Pr = 7$

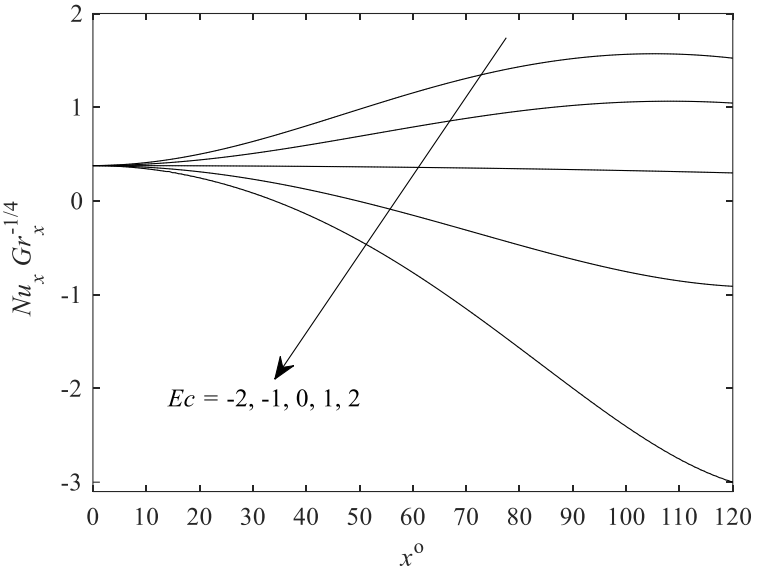

Fig. 9. Variation of $Nu_x Gr_x^{-1/4}$ for several values of Ec when $\lambda = \lambda_2 = 0.5,\ N = Nb = Nt = 0.1,\ Le = 10$ and $\Pr = 7$

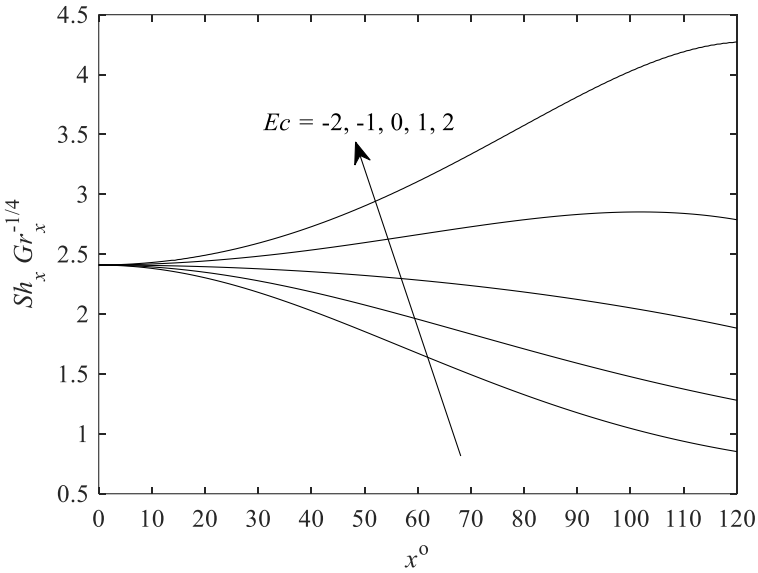

Fig. 10. Variation of $Sh_x Gr_x^{-1/4}$ for several values of Ec when $\lambda = \lambda_2 = 0.5,\ N = Nb = Nt = 0.1,\ Le = 10$ and $\Pr = 7$

4. Conclusions

The free convection boundary layer flow problem of Jeffrey nanofluid on a horizontal circular cylinder with viscous dissipation effect was deliberated. The effects of Jeffrey fluid parameter and viscous dissipation on the velocity, temperature, and concentration profiles as well as the reduced skin friction coefficient, Nusselt number and Sherwood number have been discussed and explained. Overall, the concise outcome of this investigation is provided as follows:

i. The similar distribution shows the opposite behaviour for both Jeffrey fluid parameters.

ii. An increase in Ec shows no effects on the velocity, temperature, and concentration profiles at the lower stagnation point. Augmenting Ec has enlarged the skin friction coefficient and Sherwood number, but reduced the Nusselt number.

iii. The increase of λ, λ_2 and Ec has delayed the boundary layer separation up to $x = 120°$.

Acknowledgement
This project has been supported by Ministry of Higher Education under The Fundamental Research Grant Scheme for Research Acculturation of Early Career Researchers (FRGS-RACER) (Ref:RACER/1/2019/STG06/UMP//1) through RDU192602 and Universiti Malaysia Pahang through RDU182307.

References

[1] Merkin, J.H. "Free convection boundary layer on an isothermal horizontal cylinder." In *Proceedings of the ASME-AIChE, Heat Transfer Conference,* p. 1-4.

[2] Merkin, J.H. "Free convection boundary layers on cylinders of elliptic cross section." *Journal of Heat Transfer* 99, no. 3 (1977): 453-457. https://doi.org/10.1115/1.3450717

[3] Ingham, D.B. and Pop, I. "Natural convection about a heated horizontal cylinder in a porous medium." *Journal of Fluid Mechanics* 184, (1987): 157-181. https://doi.org/10.1017/S0022112087002842

[4] Merkin, J.H. and Pop, I. "A note on the free convection boundary layer on a horizontal circular cylinder with constant heat flux." *Wärme-und Stoffübertragung* 22, no. 1-2 (1988): 79-81. https://doi.org/10.1007/BF01001575

[5] Nazar, R., Amin, N., and Pop, I. "Free convection boundary layer on an isothermal horizontal circular cylinder in a micropolar fluid." *Heat Transfer* 2 (2002): 525-530. https://doi.org/10.1615/IHTC12.2030

[6] Molla, M.M., Hossain, M.A., and Gorla, R.S.R. "Natural convection flow from an isothermal horizontal circular cylinder with temperature dependent viscosity." *Heat and Mass Transfer* 41, no. 7 (2005): 594-598. https://doi.org/10.1007/s00231-004-0576-7

[7] Molla, M.M., Hossain, M.A., and Paul, M.C. "Natural convection flow from an isothermal horizontal circular cylinder in presence of heat generation." *International Journal of Engineering Science* 44, no. 13 (2006): 949-958. https://doi.org/10.1016/j.ijengsci.2006.05.002

[8] Salleh, M.Z. and Nazar, R. "Free convection boundary layer flow over a horizontal circular cylinder with Newtonian heating." *Sains Malaysiana* 39, no. 4 (2010): 671-676.

[9] Azim, N.H.M.A. and Chowdhury, M.K. "MHD-conjugate free convection from an isothermal horizontal circular cylinder with joule heating and heat generation." *Journal of Computational Methods in Physics* 2013, (2013): 1-11. https://doi.org/10.1155/2013/180516

[10] Prasad, V.R., Gaffar, S.A., Reddy, E.K., and Bég, O.A. "Flow and heat transfer of Jeffreys non-Newtonian fluid from horizontal circular cylinder." *Journal of Thermophysics and Heat Transfer* 28, no. 4 (2014): 764-770. https://doi.org/10.2514/1.T4253

[11] Makanda, G., Shaw, S., and Sibanda, P. "Effects of radiation on MHD free convection of a Casson fluid from a horizontal circular cylinder with partial slip in non-Darcy porous medium with viscous dissipation." *Boundary Value Problems* 2015, no. 1 (2015): 75. https://doi.org/10.1186/s13661-015-0333-5

[12] Mohamed, M.K.A., Noar, N.A.Z.M., Salleh, M.Z., and Ishak, A. "Free convection boundary layer flow on a horizontal circular cylinder in a nanofluid with viscous dissipation." *Sains Malaysiana* 45, no. 2 (2016): 289-296.

[13] Rao, A.S., Amanulla, C.H., Nagendra, N., Bég, O.A., and Kadir, A. "Hydromagnetic flow and heat transfer in a Williamson Non-Newtonian fluid from a horizontal circular cylinder with Newtonian heating." *International Journal of Applied and Computational Mathematics* 3, no. 4 (2017): 3389-3409. https://doi.org/10.1007/s40819-017-0304-x

[14] Gaffar, S.A., Prasad, V.R., and Reddy, E.K. "Magnetohydrodynamic free convection flow and heat transfer of non-Newtonian tangent hyperbolic fluid from horizontal circular cylinder with Biot number effects." *International Journal of Applied and Computational Mathematics* 3, no. 2 (2017): 721-743. https://doi.org/10.1007/s40819-015-0130-y

[15] Dalir, N. "Numerical study of entropy generation for forced convection flow and heat transfer of a Jeffrey fluid over a stretching sheet." *Alexandria Engineering Journal* 53, no. 4 (2014): 769-778. https://doi.org/10.1016/j.aej.2014.08.005
[16] Hayat, T. and Ali, N. "Peristaltic motion of a Jeffrey fluid under the effect of a magnetic field in a tube." *Communications in Nonlinear Science and Numerical Simulation* 13, no. 7 (2008): 1343-1352. https://doi.org/10.1016/j.cnsns.2006.12.009
[17] Qasim, M. "Heat and mass transfer in a Jeffrey fluid over a stretching sheet with heat source/sink." *Alexandria Engineering Journal* 52, no. 4 (2013): 571-575. https://doi.org/10.1016/j.aej.2013.08.004
[18] Mohamed, M.K.A., Salleh, M.Z., Noar, N., and Ishak, A. "The viscous dissipation effects on the mixed convection boundary layer flow on a horizontal circular cylinder." *Jurnal Teknologi* 78, no. 4-4 (2016): 73-79. https://doi.org/10.11113/jt.v78.8304
[19] Azim, N.H.M. and Chowdhury, M.K. "MHD-conjugate free convection from an isothermal horizontal circular cylinder with joule heating and heat generation." *Journal of Computational Methods in Physics* 2013, (2013): 1-11. https://doi.org/10.1155/2013/180516